Density functional for hard hyperspheres from a tensorial-diagrammatic series

Gavin Leithall[1] and Matthias Schmidt[1,2]

[1]*H. H. Wills Physics Laboratory, University of Bristol, Royal Fort, Tyndall Avenue, Bristol BS8 1TL, United Kingdom*
[2]*Theoretische Physik II, Universität Bayreuth, D-95440 Bayreuth, Germany*

We represent the free energy functional by a diagrammatic series with tensorial coefficients indexed by powers of the length scale. For hard cores, we obtain Percus's exact functional in one dimension and the Kierlik-Rosinberg form of fundamental measures theory in three dimensions. In five dimensions, the functional describes bulk fluids better than does the Percus-Yevick theory. At planar walls, density profiles oscillate with smaller periods than in lower dimensions. Our findings open up avenues for treating both more general high-dimensional systems and three-dimensional mixtures via dimensional reduction.

Investigation of the effects of interparticle hard core repulsion has provided significant insights into the interfacial and capillary (phase) behavior of simple and complex liquids [1]. Recent examples include studies of ion-specific excluded-volume correlations and solvation forces [2] and the wetting properties of a solid substrate by a "civilized" model of ionic solutions [3]. Density functional theory (DFT) [4] is a primary tool for the investigation of such situations. Application of DFT requires one to have an approximation for the central (and, in general, unknown) Helmholtz free energy as a functional of the one-body density distributions $\rho_i(\mathbf{r})$ of all species i; $\mathbf{r}$ is the spatial coordinate. One such example, which has become a cornerstone of DFT, is Rosenfeld's fundamental-measure theory (FMT) [5–8] for additive hard sphere mixtures.

There is considerable current interest in the study of the hard sphere model in large space dimensions D. Motivation for such work originates from a desire to develop and gain new insights into the general structure of liquid state theories, as well as from the question of whether anything is special about $D = 3$. Studies that exemplify this strategy include investigations of fluid structure [9–12] and of freezing [13–15].

Much less is known about inhomogeneous hypersphere fluids. In this paper, we present a formalized framework for a generic hard hypersphere density functional. Its structure is based on a density series, where the central approximation lies in the starlike topology of the integral kernels that couple the field points together [see Eq. (3)].

The lowest order contribution to the exact virial expansion of the excess (over ideal gas) free energy functional is $-k_B T \int d\mathbf{r}_1 \rho_i(\mathbf{r}_1) \int d\mathbf{r}_2 \rho_j(\mathbf{r}_2) f_{ij}(|\mathbf{r}_1 - \mathbf{r}_2|)/2$, where the Mayer bond $f_{ij}(r)$ for hard spheres as a function of distance r is $f_{ij}(r) = -1$, if the two spheres with radii R_i and R_j overlap, and zero otherwise; k_B is the Boltzmann constant; and T is temperature. Graphically this can be represented by two filled dots (with each one corresponding to one multiplication by density and one integration) that are joined by a line which stands for $f_{ij}(r)$. The Kierlik-Rosinberg (KR) deconvolution of the Mayer bond for arbitrary (odd) D is $f_{ij}(|\mathbf{r}_1 - \mathbf{r}_2|) = -\sum_{\mu=0}^{D} \int d\mathbf{x} w_\mu^i(|\mathbf{r}_1 - \mathbf{x}|) w_{D-\mu}^j(|\mathbf{r}_2 - \mathbf{x}|)$, with species-dependent geometric "weight" functions $w_\mu^i(r)$; all Greek indices run from 0 to D here and in the following. Hence, diagrammatically,

$$-\frac{1}{2}\sum_{ij} \overset{i}{\bullet}\overset{f_{ij}}{\rule{2cm}{0.4pt}}\overset{j}{\bullet} = \frac{1}{2}\sum_{ij}\sum_{\mu,\nu=0}^{D} \overset{i}{\bullet}\underset{\mu}{\rule{1cm}{0.4pt}}\overset{M^{\mu\nu}}{\times}\underset{\nu}{\rule{1cm}{0.4pt}}\overset{j}{\bullet} \equiv \frac{1}{2}\bullet\overset{\mathsf{M}}{\rule{1cm}{0.4pt}\times\rule{1cm}{0.4pt}}\bullet , \tag{1}$$

where the cross indicates the position $\mathbf{x}$ with integration and the bonds labeled μ and ν represent $w_\mu^i(|\mathbf{r}_1 - \mathbf{x}|)$ and $w_\nu^j(|\mathbf{r}_2 - \mathbf{x}|)$, respectively. The second-rank tensor M has components $M^{\mu\nu} = M_{\mu\nu} = 1$ for $\mu + \nu = D$, and is zero otherwise [16]. The third diagram in (1) is a shorthand notation, where, e.g., the first bond, together with its filled circle, represents $\sum_i \int d\mathbf{r}_1 \rho_i(\mathbf{r}_1) w_\mu^i(|\mathbf{r}_1 - \mathbf{x}|) \equiv n_\mu(\mathbf{x})$; tensor

contraction over all Greek indices is implied. Both w_μ^i and n_μ possess units of (length)$^{\mu-D}$. In $D = 3$, the $n_\mu(\mathbf{x})$ are the familiar KR weighted densities [6], if the corresponding form of the $w_\mu^i(r)$ is used.

We approximate the exact "triangle diagram" of third order [17] by a three-arm star:

$$-\frac{1}{6}\sum_{ijk} \triangle_{f_{ij}}^{f_{ik}\ k\ f_{jk}} \approx \frac{1}{6}\sum_{ijk}\sum_{\mu,\nu,\tau=0}^{D} \overset{\tau}{\underset{\mu\ \ \nu}{\times}}^{J^{\mu\nu\tau}\ k} \equiv \frac{1}{6}\,\mathsf{J}\text{-star} , \tag{2}$$

where the third-rank tensor J has components $J^{\mu\nu\tau}$, which we assume (i) to be symmetric under exchange of indices, (ii) to satisfy $J^{D\mu\nu} = M^{\mu\nu}$, and (iii) to vanish if $\mu + \nu + \tau \neq 2D$, because the diagram has to be of dimension (length)^0.

Restricting ourselves to star topology, we assume the excess free energy functional in D dimensions to have the generic form

$$\beta\mathcal{F}_{\text{exc}}[\{\rho_i\}] = \frac{1}{2}\bullet\!\!-\!\!\overset{M}{\times}\!\!-\!\!\bullet + \frac{1}{6}\,\overset{J}{\wedge} + \frac{1}{12}\,\overset{JJ}{\times} + \frac{1}{20}\,\underset{JJJ}{\asymp} + \cdots, \quad (3)$$

where $\beta = 1/(k_B T)$, and the scalar coefficients are taken from the zero-dimensional excess free energy $\varphi_0(\eta) = (1-\eta)\ln(1-\eta) + \eta = \sum_{k=2}^{\infty} \eta^k/[k(k-1)] = \eta^2/2 + \eta^3/6 + \eta^4/12 + \cdots$; here η is a dummy variable. The product JJ indicates tensor contraction via $\sum_{\tau=0}^{D} J^{\mu\nu\tau} J_\tau{}^{\kappa\lambda}$, where $J_\tau{}^{\kappa\lambda} = \sum_{\tau'=0}^{D} M_{\tau\tau'} J^{\tau'\kappa\lambda}$; the triplet JJJ represents $\sum_{\tau,\sigma=0}^{D} J^{\mu\nu\tau} J_\tau{}^{\kappa\sigma} J_\sigma{}^{\iota\zeta}$; etc. In order to find a closed expression for (3), we define a matrix of weighted densities,

$$N(x) = \overset{\bullet}{\underset{\times}{\big|}}\, J, \quad (4)$$

where the spatial argument $\mathbf{x}$ is not integrated over. The components of $N(\mathbf{x})$ are $N_\mu{}^\nu(\mathbf{x}) = \sum_i \sum_{\tau=0}^{D} J_\mu{}^{\nu\tau}(w_\tau^i * \rho_i)(\mathbf{x})$, where $*$ denotes the D-dimensional convolution $(g * h)(\mathbf{x}) = \int d\mathbf{r}\, g(\mathbf{x} - \mathbf{r}) h(\mathbf{r})$ of the two functions $g(\mathbf{x})$ and $h(\mathbf{x})$. The definition (4) allows one to express the kth order diagram in (3) as a matrix power $N(\mathbf{x})^k$ with integration over $\mathbf{x}$. Subsequently one has to take the appropriate component $\mu = 0$, $\nu = D$ [18]. Hence we can view (3) as one component of the tensorial functional

$$\beta\mathsf{F}_{\text{exc}}[\{\rho_i\}] \equiv \int d\mathbf{x} \sum_{k=2}^{\infty} \frac{N(\mathbf{x})^k}{k(k-1)} = \int d\mathbf{x}\, \varphi_0(N(\mathbf{x})), \quad (5)$$

where the second equality comes from using the Taylor series of $\varphi_0(\eta)$. The physically relevant functional $\mathcal{F}_{\text{exc}}[\{\rho_i\}]$ is the $\mu = 0$, $\nu = D$ component, i.e., $\mathcal{F}_{\text{exc}} = (\mathsf{F}_{\text{exc}})_0{}^D$, which can be written as $\beta\mathcal{F}_{\text{exc}}[\{\rho_i\}] = \int d\mathbf{x}\,\Phi$, where the free energy density $\Phi = [\varphi_0(N(\mathbf{x}))]_0{}^D$.

All properties specific to the value of D are entirely encapsulated (i) in the dimensionality of the space integrals, (ii) in the prescription of the $D + 1$ weight functions $w_\mu^i(r)$, and (iii) in the choice of the (constant) components $J^{\mu\nu\tau}$ of J. For all $D > 0$, we use $w_D^i(r) = \Theta(r - R_i)$ and $w_{D-1}^i(r) = \delta(r - R_i)$, where $\Theta(\cdot)$ is the Heaviside (unit step) function and $\delta(\cdot)$ is the Dirac delta distribution. For all cases considered, we could obtain the specific form of the further weight functions and the form of J from the minimalistic requirement that the two-body bulk fluid direct correlation function $c_{ij}(|\mathbf{r} - \mathbf{r}'|) = -\delta^2\beta F_{\text{exc}}/\delta\rho_i(\mathbf{r})\delta\rho_j(\mathbf{r}')|_{\rho_k=\text{const}}$ is free of divergences, i.e.,

$$|c_{ij}(r)| < \infty \quad \text{for all } r. \quad (6)$$

In $D = 1$, $J^{011} = 1$ determines J entirely and straightforward algebra yields $\beta\mathcal{F}_{\text{exc}} = -\int d\mathbf{x}\, n_0(\mathbf{x})\ln[1 - n_1(\mathbf{x})]$, which is exact [19,20]. In $D = 3$ we use the KR form for the additional weight functions $w_1^i(r)$ and $w_0^i(r)$, and

obtain $J^{033} = J^{123} = 1$, $J^{222} = 1/(4\pi)$, which gives the KR functional [6]. In $D = 5$ we obtain

$$\Phi = -n_0\ln(1 - n_5) + \frac{n_1 n_4 + n_2 n_3}{1 - n_5} + \frac{n_2 n_4^2 + n_3^2 n_4/(64\pi^2)}{(1 - n_5)^2}$$
$$+ \frac{n_3 n_4^3}{48\pi^2(1 - n_5)^3} + \frac{n_4^5}{160\pi^2(1 - n_5)^4}, \quad (7)$$

with the weight functions $w_5^i = \Theta(R_i - r)$, $w_4^i = \delta(R_i - r)$, $w_3^i = \delta'$, $w_2^i = \delta'/(16\pi^2 r)$, $w_1^i = (8r^{-1}\delta'' - \delta''')/(64\pi^2)$, and $w_0^i = (24r^{-3}\delta' + 24r^{-2}\delta'' - 12r^{-1}\delta''' + \delta'''')/(64\pi^2)$, where $\delta'(R_i - r), \ldots, \delta''''(R_i - r)$ denote successive derivatives of the Dirac δ function; the arguments have been omitted for clarity.

For constant density fields, the five-dimensional (5D) functional yields an analytical excess free energy for bulk fluids, $F_{\text{exc}}(\{\rho_i\}) = \mathcal{F}_{\text{exc}}[\{\rho_i = \text{const}\}]$. When scaled as $\beta F_{\text{exc}}/V$, this equals (7), but with $n_\mu = \sum_i \xi_\mu^i \rho_i = \text{const}$, where the
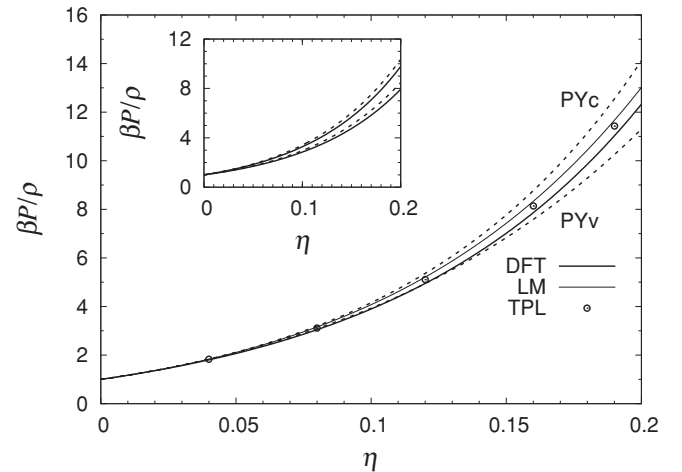

FIG. 1. Compressibility factor $\beta P/\rho$ as a function of packing fraction η for 5D hard hyperspheres, as obtained from the DFT bulk free energy (thick line), and compared to the PY compressibility (PYc) and virial (PYv) results (dashed lines) and the LM (thin line) equation of state [9]. Also shown are DFT results from the test particle limit (TPL, symbols) using the virial theorem. The inset shows $\beta P/\rho$ as a function of the total packing fraction $\eta \equiv n_5$ for binary mixtures of 5D hard hyperspheres as obtained from DFT (solid lines), along with the equation of state of Ref. [10] (dashed lines). The upper pair of curves is for size ratio 4 and composition 0.75 of the larger species; the lower pair of curves is for an equimolar mixture with size ratio 2.5.
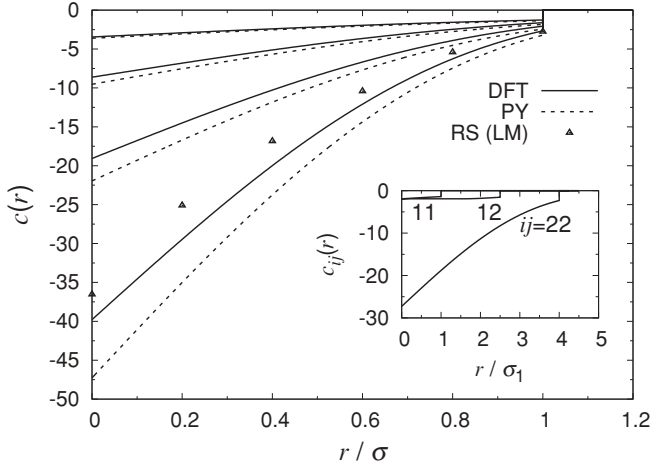
FIG. 2. Bulk two-body direct correlation function $c(r)$ as a function of the scaled distance r/σ, for 5D hard hyperspheres, as obtained from DFT via the second functional derivative (solid lines), along with the PY result (dashed lines), for packing fractions $\eta = 0.05, 0.1, 0.15, 0.2$ (from top to bottom). Also shown is the result of the theory by Rohrmann and Santos (RS) [11] (symbols), which is based on the LM equation of state [9], for $\eta = 0.2$ (we omit the small, positive Yukawa tail outside of the core). The inset shows DFT results for the partial pair direct correlation functions $c_{ij}(r)$ as a function of r/σ_1, where $\sigma_1 = 2R_1$ for a binary mixture of 5D hard hyperspheres with size ratio 4, composition of 0.75 for the (larger) species 2, and total density $\rho\sigma_1^5 = 1.4$, corresponding to $\eta = 0.173$ (cf. inset of Fig. 1).

fundamental measures $\xi_\mu^i = \int d\mathbf{r}\, w_\mu^i(\mathbf{r})$ are $\xi_0^i = 1$, $\xi_1^i = R_i$, $\xi_2^i = R_i^2/2$, $\xi_3^i = 32\pi^2 R_i^3/3$, $\xi_4^i = 8\pi^2 R_i^4/3$, and $\xi_5^i = 8\pi^2 R_i^5/15$. The total packing fraction is simply $\eta \equiv n_5$. The pressure is obtained from $P = -\partial F_{\text{exc}}/\partial V + k_B T\rho$, where $\rho = \sum_i \rho_i$. Figure 1 shows $\beta P/\rho$ for pure 5D
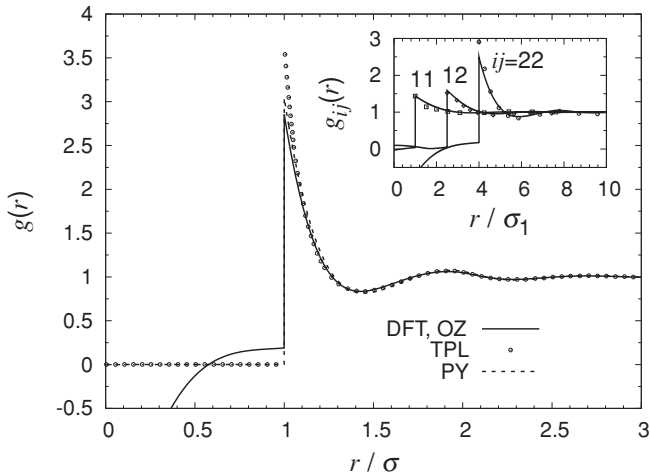

FIG. 3. The radial distribution function $g(r)$ as a function of r/σ, for 5D hard hyperspheres, as obtained from DFT using the OZ equation (solid line) and the test particle method (symbols), and compared with the PY result (dashed line), for packing fraction $\eta = 0.2$. The OZ result reaches $g(0) = -2.82$ at zero separation. The inset shows the partial pair distribution functions $g_{ij}(r)$ as obtained from the OZ method (lines) for the binary mixture described in the inset of Fig. 2, along with simulation results [12] (symbols).

hard hyperspheres as a function of η. The DFT result lies between the two Percus-Yevick (PY) equations of state; these deviate more strongly from each other than in three dimensions. Moreover, DFT only slightly underestimates, over the full range of (fluid) packing fractions, the semiempirical Luban-Michels (LM) equation of state [9], which yields excellent agreement with simulation data. For two representative binary mixtures (see inset of Fig. 1), DFT slightly underestimates the very accurate equation of state of Ref. [10], with similar (small) deviations as in the pure case.

Figure 2 shows the pair direct correlation function $c(r)$ for the pure 5D hard hypersphere fluid. Outside of the core, the direct correlation function vanishes, $c(r > \sigma) = 0$, and it is a fifth-order polynomial in r for $r < \sigma$, similar to the PY result; $\sigma = 2R$ is the particle diameter. However, the DFT result is smaller in magnitude than in the PY theory. This constitutes an improvement, as can be observed by comparing it with
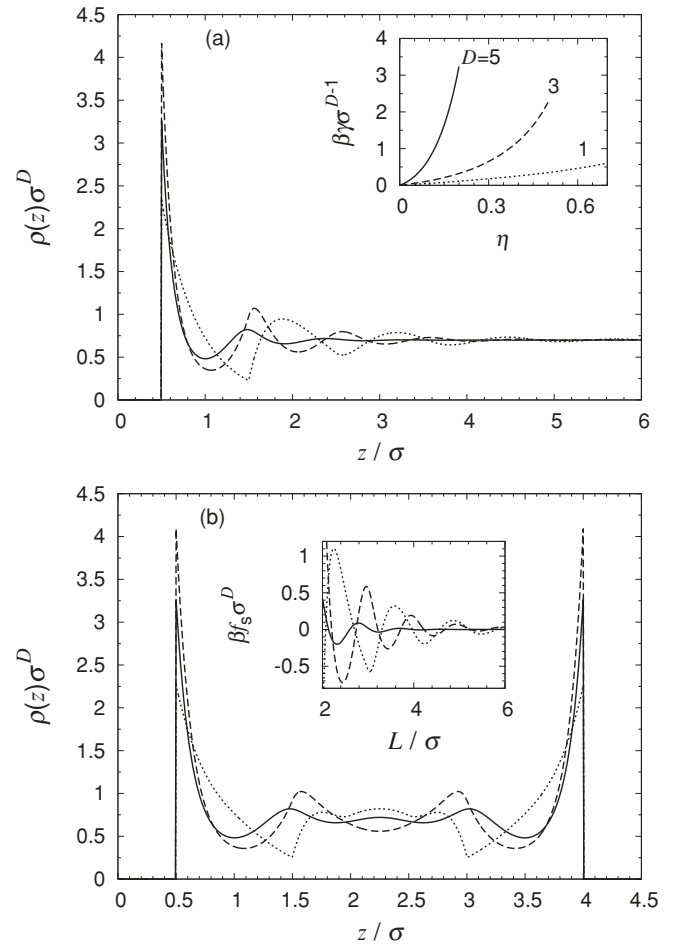

FIG. 4. Scaled density profiles $\rho(z)\sigma^D$ as a function of the scaled distance z/σ for packing fraction $\eta = 0.7$ in 1D (dotted line), $\eta = 0.367$ in 3D (dashed line), and $\eta = 0.115$ in 5D (solid line). (a) Hard hypersphere fluids adsorbed at a hard wall; z is the distance from the wall. The inset shows the surface tension $\beta\gamma\sigma^{D-1}$ due to the presence of the wall as a function of η. (b) Density distributions for hard hypersphere fluids in a planar slit with width $L = 4.5\sigma$ in chemical equilibrium with a bulk having the same value of η as given above. The inset shows the scaled solvation force $\beta f_S\sigma^D$ as a function of L/σ.

the sophisticated theory by Rohrmann and Santos (RS) [11], which is built on the LM equation of state. For $\eta = 0.2$, a value higher than that at freezing [13], we find that, indeed, the DFT result deviates much less from the RS theory than does the PY result. The inset of Fig. 2 shows an example of partial pair direct correlation functions, calculated from the functional. As expected, these satisfy $c_{ij}(r > R_i + R_j) = 0$ and they are free of divergences.

Figure 3 displays corresponding results for the radial distribution function $g(r)$, obtained from the Ornstein-Zernike (OZ) relation with $c(r)$ as input. Outside of the core, the deviation between the PY and DFT results is very small, but the contact value from DFT is lower and some core violation is apparent. We also show results from a test particle calculation, where we have numerically minimized the density functional in the presence of an external potential that equals the pair interaction potential. Here the core condition is automatically satisfied. The contact value $g(\sigma^+)$ increases and becomes larger than the PY value. When input into the virial theorem $\beta P/\rho = 1 + 2^{D-1}\eta g(\sigma^+)$, the result is almost indistinguishable (see Fig. 1) from the quasiexact LM result. The inset of Fig. 3 shows the partial pair distribution functions $g_{ij}(r)$ for the mixture considered above (inset of Fig. 2). The agreement with simulation results [12] is excellent. Hence DFT gives a very good account of both the thermodynamics and the structure of pure and binary bulk liquids of 5D hard hyperspheres.

Density profiles at a hard wall are shown in Fig. 4(a) for the 1D, 3D, and 5D cases, keeping the scaled bulk density $\rho\sigma^D = 0.7 = $ const. With increasing dimensionality, the distance between the liquid layers that are induced by the wall decreases strongly. The surface tension $\gamma = (\Omega + pV)/A$, where Ω is the grand potential, A is the area of the wall, and V is the system volume $z \geqslant 0$, is shown in the inset of Fig. 4(a) [21]. This is seen to rise much more strongly with η for increasing D. Figure 4(b) shows density profiles in a slit for 1D (hard rods on a line), 3D, and 5D. Again very different structuring is apparent, with the position of the secondary peaks being closest

to the wall for 5D and five (four) layers present in 5D (3D). The inset of Fig. 4(b) shows the solvation force $\beta f_S(L)$, which for hard walls can be obtained from $\beta f_S(L) = \rho(\sigma^+/2) - \beta P$, as a function of the slit width L. This again highlights the sensitive dependence on dimensionality.

Our formalized diagrammatic approach to DFT has significant relevance for future developments:

(i) A whole class of FMT functionals for 3D models can be generalized in a straightforward way to high dimensions. This includes the penetrable sphere model of particles interacting with a repulsive step function pair potential [22] [via adapting the scalar coefficients in Eq. (3) in order to allow for thermally induced overlap of particles], the Asakura-Oosawa colloid-polymer mixture [23] (via linearizing the hypersphere mixtures functional in one of the densities, which then describes an ideal polymer species), and the Widom-Rowlinson model [24] [via using the appropriate expression for the zero-dimensional free energy in order to generate the scalar coefficient in Eq. (3)].

(ii) Novel functionals for 3D models can be obtained via dimensional *reduction*, where the hard hypersphere functional [or one of its descendants described in (i)] is exposed to dimensional crossover, such that the density distribution is assumed to be a δ function (or superposition of several δ functions) in one or more space dimensions. The particles in each hyperspace then constitute an individual species in 3D. Mixtures with negative nonadditivity can be obtained via this procedure; see, e.g., Ref. [25] for a corresponding example of crossover from 3D to 2D.

(iii) Although we have used the KR approach, very interesting and useful further insights could be gained from generalizing Rosenfeld's more geometric formulation [5] to high dimensions. This also applies to its refinements based on consideration of zero-dimensional cavities [26,27], possibly following the initial steps taken in Ref. [15].

[1] R. Evans, J. Phys. Condens. Matter **2**, 8989 (1990).

[2] I. Kalcher, J. C. F. Schulz, and J. Dzubiella, Phys. Rev. Lett. **104**, 097802 (2010).

[3] A. Oleksy and J. P. Hansen, J. Chem. Phys. **132**, 204702 (2010).

[4] R. Evans, Adv. Phys. **28**, 143 (1979).

[5] Y. Rosenfeld, Phys. Rev. Lett. **63**, 980 (1989).

[6] E. Kierlik and M. L. Rosinberg, Phys. Rev. A **42**, 3382 (1990).

[7] P. Tarazona, J. A. Cuesta, and Y. Martinez-Raton, in *Theory and Simulation of Hard-Sphere Fluids and Related Systems*, edited by A. Mulero, Lecture Notes in Physics Vol. 753 (Springer, Berlin, 2008).

[8] R. Roth, J. Phys. Condens. Matter **22**, 063102 (2010).

[9] M. Luban and J. P. J. Michels, Phys. Rev. A **41**, 6796 (1990).

[10] A. Santos, S. B. Yuste, and M. López de Haro, Mol. Phys. **99**, 1959 (2001).

[11] R. D. Rohrmann and A. Santos, Phys. Rev. E **76**, 051202 (2007).

[12] M. González-Melchor, J. Alejandre, and M. López de Haro, J. Chem. Phys. **114**, 4905 (2001).

[13] J. A. van Meel, B. Charbonneau, A. Fortini, and P. Charbonneau, Phys. Rev. E **80**, 061110 (2009).

[14] J. L. Colot and M. Baus, Phys. Lett. A **119**, 135 (1986).

[15] R. Finken, M. Schmidt, and H. Löwen, Phys. Rev. E **65**, 016108 (2001).

[16] M. Schmidt and M. R. Jeffrey, J. Math. Phys. **48**, 123507 (2007).

[17] The rapid convergence of the virial series with increasing dimensionality is true only for homogeneous (bulk) fluid states.

[18] Taking this component corrects for having k factors of J in $\mathsf{N}(\mathbf{x})^k$, but only $k-2$ such factors in the kth-order diagram in (3).

[19] J. K. Percus, J. Stat. Phys. **15**, 505 (1976).

[20] T. K. Vanderlick, H. T. Davis, and J. K. Percus, J. Chem. Phys. **91**, 7136 (1989).

[21] We have numerically tested that $\beta P = \rho(\sigma^+/2)$ and $-\partial\gamma/\partial\tilde{\mu} = \int dz[\rho(z) - \rho(\infty)]$, where $\tilde{\mu}$ is the chemical potential, are satisfied. For the slit, we have checked $f_S = -2(\partial\gamma/\partial L)_{\tilde{\mu},A}$.

[22] M. Schmidt, J. Phys. Condens. Matter **11**, 10163 (1999).

[23] M. Schmidt, H. Löwen, J. M. Brader, and R. Evans, Phys. Rev. Lett. **85**, 1934 (2000).

[24] M. Schmidt, Phys. Rev. E **63**, 010101(R) (2000).

[25] Y. Rosenfeld, M. Schmidt, H. Löwen, and P. Tarazona, Phys. Rev. E **55**, 4245 (1997).

[26] P. Tarazona and Y. Rosenfeld, Phys. Rev. E **55**, R4873 (1997).

[27] P. Tarazona, Phys. Rev. Lett. **84**, 694 (2000).